THESIS

ASSESSING THE USE OF DUAL-DRAINAGE MODELING TO DETERMINE THE EFFECTS OF GREEN STORMWATER INFRASTRUCTURE NETWORKS ON EVENTS OF ROADWAY FLOODING

Submitted by

Kathryn Knight

Department of Civil and Environmental Engineering

In partial fulfillment of the requirements

For the Degree of Master of Science

Colorado State University

Fort Collins, Colorado

Summer 2020

Master's Committee:

Advisor: Aditi Bhaskar

Mazdak Arabi
Stephanie Kampf

ABSTRACT

ASSESSING THE USE OF DUAL-DRAINAGE MODELING TO DETERMINE THE EFFECTS OF GREEN STORMWATER INFRASTRUCTURE NETWORKS ON EVENTS OF ROADWAY FLOODING

Roadway flooding occurs when a stormwater network does not have the capacity to drain all runoff generated by precipitation. Roadway flooding causes damage to infrastructure and property, risks to human health and safety, and disruptions to transportation systems. Green stormwater infrastructure (GSI) has been increasingly used to reduce stormwater input to the subsurface stormwater network, stormwater draining to urban streams, and to improve water quality. It is unclear how GSI interacts with surface runoff and stormwater structures to affect the spatial extent and distribution of roadway flooding. This interaction was explored using a dual drainage model with individual stormwater structures represented, fine spatial resolution, and bidirectional flow between the subsurface stormwater network and surface runoff. The model was developed using the Stormwater Management Model for PC (PCSWMM) in the urban watershed Harvard Gulch in Denver, Colorado. We examined how dual drainage modeling could reveal the effect of converting between 1% and 5% of directly connected impervious area (DCIA) in the watershed to bioretention GSI on the extent, depth, and distribution of roadway flooding. Results of the surface flooding model were generally co-located with resident reports related to flooding within the study area. Results show that even for 1% of DCIA converted to GSI, the extent and mean depth of roadway flooding was reduced for the duration of the simulation, and increasing GSI conversion further reduced roadway flooding

depth and extent. We found diminishing returns in the roadway flood extent reduction per additional percentage of DCIA converted to GSI beyond 2.5%, whereas diminishing returns occurred beyond 1% conversion to GSI for mean roadway flood depth reduction. This work also examined the limitations to the accurate representation of roadway flooding due to incomplete input data, a lack of observational data for urban floods, GSI placement methods, and high computational demands. With future work to reduce limitations, detailed dual drainage modeling has the potential to better predict what strategies will mitigate roadway flooding.

ACKNOWLEDGEMENTS

Foremost, I would like to thank my advisor, Dr. Aditi Bhaskar, for the support and expertise she has shared that have helped me find direction through the challenges of completing this project. I would also like to thank my committee, Dr. Stephanie Kampf and Dr. Mazdak Arabi for their valuable input and perspective in the completion of this project. Additionally, I would like to acknowledge Connor Williams for his assistance in compiling observational datasets.

I would additionally like to acknowledge the Computation Hydraulics International for their support through technology grants and access to PCSWMM software. As well as Matrix Design group for providing valuable background information and stormwater modeling that supported this project. The work presented in this thesis was conducted with support from Colorado State University, the Mountain-Plains Consortium, a University Transportation Center funded by the U.S. Department of Transportation, and the Colorado Water Center.

TABLE OF CONTENTS

CHAPTER 1 - INTRODUCTION

The increase in impervious surfaces characteristic of urbanization leads to higher peak runoff and total runoff volume in receiving water bodies (Shuster et al. 2005). These effects of urbanization indicate a loss of the watershed's ability to naturally mitigate flooding and must be compensated for by the implementation of stormwater management practices (Lee et al. 2012). These stormwater management practices are commonly still inadequately sized, designed, or maintained to mitigate the frequency and magnitude of floods in urban watersheds (Perez-Pedini et al. 2005; Zellner et al. 2016). It has been shown that climate change has increased, and will likely continue to increase, the magnitude, intensity, and frequency of precipitation events, especially in the central United States (Field et al. 2012). These climate change impacts will further increase strain on stormwater systems to mitigate runoff and prevent urban flooding.

Urban flooding is caused by ageing, inadequate, or damaged stormwater systems that are unable to mitigate runoff during a storm event, and results in repeated damage to property and infrastructure, economic disruption, and increased risk to human health and safety (Galloway et al. 2018; Schmitt et al. 2004). Assessment of urban flood impacts is challenging as flood events are often highly localized, may occur outside of FEMA-designated floodplains, and are often not large enough to trigger public reports to local municipalities. Survey data from 350 municipalities across the United States found that urban flooding outside of established flood plains was occurring in 85% of reporting communities (Galloway et al. 2018). Furthermore, urban flooding disproportionately affects lower-income communities as 70% of flooding occurred in low-moderate or low-income housing areas (Galloway et al. 2018). These communities are more likely to lack the resources to address ageing infrastructure or implement

new infrastructure solutions, while also being the communities where populations are most vulnerable to the impacts of property damage and economic loss.

The frequent disruption caused by smaller events of roadway flooding, called nuisance flooding, hides the cumulative impact roadway flooding has on communities and transportation systems. Nuisance flooding is characterized by flood depths below 30-60 cm (1-2 ft) (Jacobs et al. 2018), but roadways are considered impassable or partially impassable (e.g., a single lane is inundated) when flood depths exceed 30 cm (1 ft), which is the average clearance height of vehicles (Pregnolato et al. 2016). Roadway flooding leads to the disruption of transportation systems even when flood depths are still passable by causing hazardous driving conditions that require a reduced safe driving speed. Because of the connectivity of traffic networks, localized roadway flooding can cause traffic disruptions that reach far beyond the extent of the flood (Pregnolato et al. 2016). These disruptions can cause significant economic loss (Jacobs et al. 2018; Schmitt et al. 2004). For example, roadway flooding causes a total of 100 million vehicle-hours of delay on the East Coast annually (Jacobs et al. 2018). The impacts of roadway flooding pose a risk to the function of transportation networks during emergency events (Pregnolato et al. 2016).

One possible strategy to mitigate roadway flooding is the implementation of green stormwater infrastructure (GSI). GSI are types of stormwater control measures (SCMs) that use infiltration or harvest to reduce the amount of water directly entering the subsurface stormwater network. Bioswales, bioretention, rain gardens, infiltration basins, green roofs, and pervious pavement are all types of infiltration-based GSI; rain barrels or rainwater harvesting are types of harvest-based GSI (Askarizadeh et al. 2015; Zellner et al. 2016). The effect of single structure or small-scale GSI networks has been widely studied and it has been shown that, depending on the

design, infiltration, and rainfall conditions, GSI can reduce and delay the peak of runoff entering into the stormwater network (Askarizadeh et al. 2015; Qin et al. 2013). At a watershed-scale, infiltration and harvest-based GSI generally increased runoff thresholds and decreased peak flow and volume (Jefferson et al. 2017). Less consensus has been established on how much impervious area needs to be converted to GSI to see reductions in peak flow and volume, or where in the watershed it is optimal to apply GSI. One study found a minimum of 5% effective impervious area converted to GSI (Palla and Gnecco 2015) reduced peak flow by 3% but did not reduce runoff volumes (Palla and Gnecco 2015). Another study determined that 10-15% of total impervious area needed to be converted to GSI to see a reduction in neighborhood-scale flooding and 20% conversion to reduce roadway flooding, after which more conversion had diminishing marginal benefit (Zellner et al. 2016).

Because of the many different options for GSI density, placement, management goals, and the reality of limited available locations for GSI construction in urban catchments, studies have used optimization methods for determining the most effective GSI network depending on desired outcomes (Lee et al. 2012; Perez-Pedini et al. 2005; Zellner et al. 2016). Zellner et al. (2016) developed a spatially-explicit process-based model called the Landscape Green Infrastructure Design model (L-GriD) that can be used to understand how GSI network placement and type impacts flooding at a neighborhood-scale. They found distributing GSI was more effective than clustering GSI, vegetated curb cuts were the most effective GSI, and that locating GSI near roads, particularly near stormwater outlets, reduced burden on stormwater systems. Perez-Pedini et al. (2005) and Zellner et al. (2016) opted to develop new models rather than utilize existing modeling because previous methods did not adequately represent the spatial

interactions between GSI, runoff, and stormwater systems over a neighborhood or catchment scale.

Distributed models, such as the EPA stormwater management model (SWMM), are often used for detailed site-scale or simplified watershed-scale stormwater models, but less often for a detailed watershed-scale because of the laborious model setup procedures and high data requirements. Simplified stormwater networks typically consist of subcatchments that are too large to capture the interactions that occur between stormwater network structures and local variations in topography, land cover, soils, or GSI placement (Zellner et al. 2016). Because of these modeling limitations, the current understanding of how individual GSI units interact with surface runoff, stormwater networks, and neighboring GSI over a larger area is unclear. Previous studies examining GSI impacts on urban flooding utilized a simplified stormwater network and examined flood volume at specific locations within the stormwater network, also called nodes (Qin et al. 2013), or in a small-scale (0.313 km^2) stormwater network using a combined index based on the flooded volume, rate, and duration at network nodes (Zhu and Chen 2017). This previous work examining GSI impacts on urban flooding however did not model urban flooding as a 2D water surface, which limits the physical understanding of how GSI affects urban systems, such as transportation networks, beyond the generalized metric of flood reduction at nodes.

An alternative method to examining node-based flooding to capture the interaction between GSI, surface runoff, and stormwater networks is utilizing dual drainage modeling. Dual drainage modeling couples a 2D surface runoff model domain and 1D subsurface stormwater network model domain and has bidirectional flow between the two modeling domains (Liwanag et al. 2018; Schmitt et al. 2004). The concept of dual drainage modeling is not new; it has for

decades been understood that the interaction between surface runoff and stormwater networks was a critical component of urban stormwater modeling (Djordjević et al. 1999). However, because of the computational demand required to model bidirectional interaction of distributed 2D surface runoff and 1D stormwater drainage systems for larger study areas, the conceptual understanding of dual drainage modeling has long outpaced the ability to execute such models . Observations of surcharge from stormwater inlets or flood depths are sparse, and even as computational advances make complex dual drainage models more accessible, the lack of observed data for comparison is a critical limitation (Elliott and Trowsdale 2007). A potential solution to a lack of calibration data for urban flooding is the use of resident reports of flooding. Resident reports of flooding in New York City, NY have been used to examine spatially variable response of urban flooding to precipitation (Smith and Rodriguez 2017). The ability of dual drainage modeling to simulate flooding caused by exceedance of the subsurface stormwater system capacity across the entire study area to represent urban roadway flooding allows us to address the following research questions:

1. How can dual drainage modeling help determine the effect of GSI networks on the depth, flooded extent, and spatial distribution of roadway flooding?
2. What are the limitations of dual drainage modeling for characterizing the effects of GSI networks on roadway flooding?

CHAPTER 2 - METHODS

2.1 Study Area and Data Sources

The study area is a 8.26 km^2 sub-basin of the Harvard Gulch watershed located in Denver, Colorado bordering Englewood, Colorado (Figure 1). This region of Colorado just east of the Rocky Mountains is characterized as a semi-arid climate and receives an average of 381 mm of precipitation per year (NOAA). Harvard Gulch was categorized as a medium to high priority basin for green infrastructure planning and improvements based water quality conditions, amount of directly connected impervious area (DCIA), redevelopment potential, Right-of-Way (ROW) imperviousness, existing treatment infrastructure, park density, and social justice/inequality in a Denver Public Works report (City and County of Denver 2018). Harvard Gulch flows east to west through the watershed, beginning as an open channel, then as a concrete trapezoidal channel, and finally as an underground rectangular conduit before draining into another open channel at Harvard Gulch park at the western limit of the study area. There are two USGS stream gages located within the study area: the upstream USGS gage 06711570 is located at Colorado Boulevard, and the downstream USGS gage 06711575 is located at Harvard Gulch Park near the western edge of the study area, and is also referred to here as the outfall.

The Harvard Gulch watershed has been the subject of research on urban watersheds since the 1990s, which has led to a wealth of background information as well as thorough monitoring of streamflow and precipitation in the watershed (Urbonas et al. 1990). Most recently, in 2016 the Matrix Design group produced a conceptual design report for the Harvard Gulch and Dry Gulch Major Drainageway Plan including hydrological modeling using EPA SWMM and hydraulic modeling with HEC-RAS and FLO-2D to examine the hydrologic and streamflow

response to rainfall of specific return periods (Matrix Design Group 2016). Information from the report was used to verify input data used to develop the stormwater model for this project, including drainage area delineations, storage curves, soil classification, flood frequency analysis, and channel geometry; as well as useful background on stormwater management in the study area. However, the previously developed model could not be directly used for purposes of this study as it does not describe structure-scale details of the stormwater network and interactions with overland flow. Rather, runoff routing was simplified to a single or small number of inlets for each subcatchment. Additionally, in order to isolate the runoff and stormwater network draining to the USGS gage 06711575 at Harvard Gulch park, the study area outfall where calibration will be performed (Figure 1), the study area of this project covers a subset of the area assessed by Matrix Design Group in 2016. The southern boundary of the study area is delineated by the Highline Canal. The Matrix report approximated that runoff from 19% of the study area examined in their model would flow into the Highline Canal rather than into Harvard Gulch. The areas determined by Matrix Design Group that drain into the Highline Canal, Dry Gulch, or downstream of the USGS Gage 06711575 were excluded from the study area of this project (Matrix Design Group 2016).

The resulting catchment area is 8.26 km^2, has an average imperviousness of 36%, and an average slope of 0.44%. The direct connected impervious area (DCIA) was estimated as 45% of the impervious area using a Denver-specific equation (Alley and Veenhuis 1983). Harvard Gulch is considered a fully developed watershed, the main land use is characterized as 51% residential (single and multi-family), 13% park/public spaces, and 5% commercial (City and County of Denver 2015). Imperviousness and land use data were collected from the City and County of Denver Open Data Catalog (City and County of Denver) and were most recently updated in

2016. The average slope was computed from the 3-meter resolution digital elevation model (DEM) from the National Elevation Dataset. There is no soil classification by the United States Department of Agriculture (USDA) Natural Resources Conservation Survey (NRCS) Web Soil Survey available for the study area. However, the adjacent neighborhood in Englewood, Colorado has a soil classification of type C, which was used as an approximate soil classification for the study area. There are five USGS rain gages located within the study area (Figure 1) with rainfall measured at 5-minute intervals.

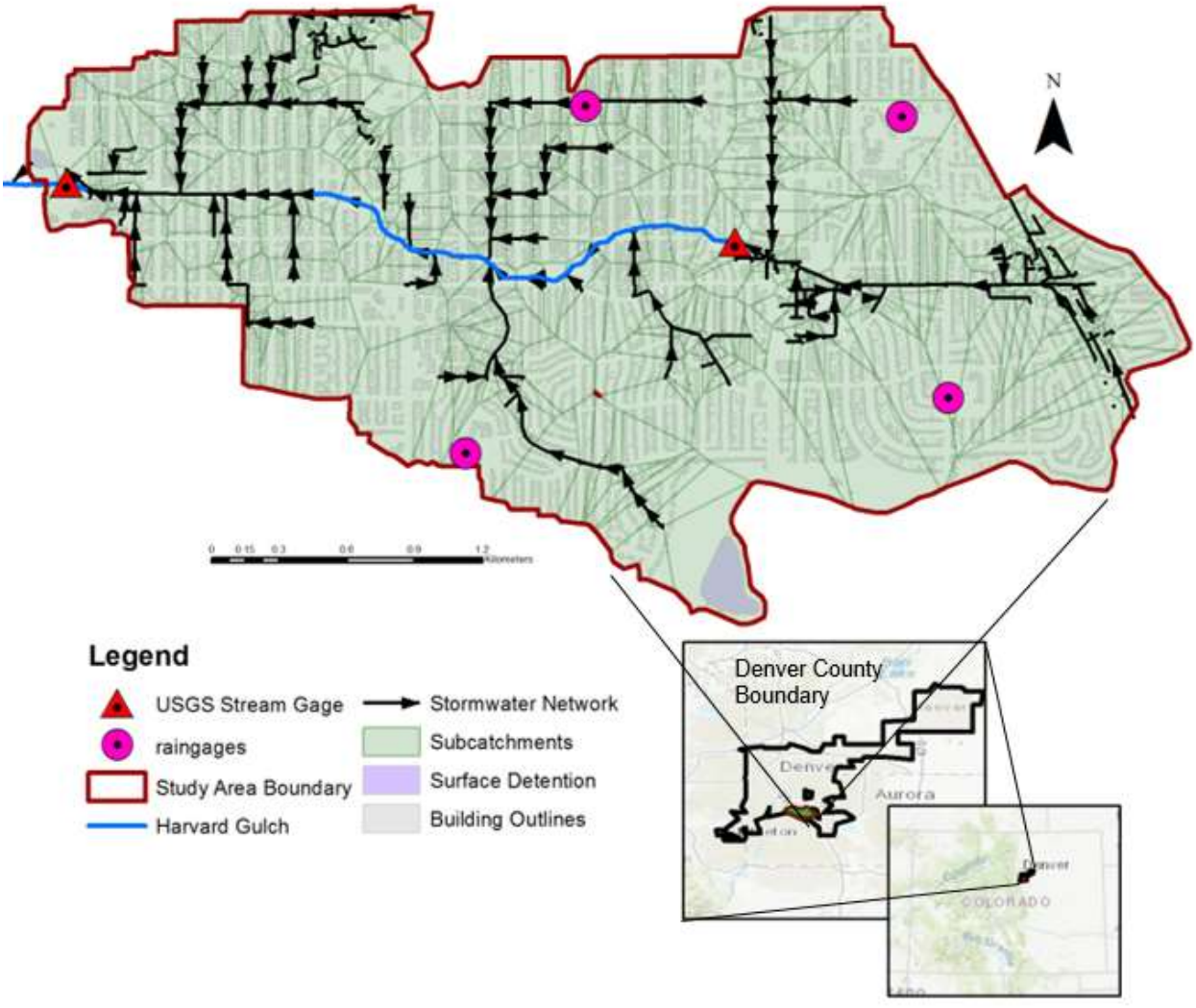

Figure 1. Study area including location of the study area outfall USGS stream gage 06711575 (left), USGS stream gage 06711570, and rain gages. The fifth rain gage is co-located at USGS stream gage 06711575.

2.2 Model Application

In order to model the interactions between overland flow and the subsurface stormwater network, a dual drainage model with major and minor system domains was developed in PCSWMM (CHI Water). The 1D subsurface stormwater network model domain, or minor system, describes the traditional subsurface stormwater network including conduits/pipes, manholes, inlets, and underground storage nodes. The 2D surface runoff model domain, or major system, describes the surface components that convey overland flow. PCSWMM is a modeling software from CHI Water that utilizes EPA SWMM5 and has functionality to model 1D minor system flows, 2D major system flows, and dynamic bidirectional interactions between the major and minor system domains necessary to model 2D roadway flooding.

2.2.1 1D Minor System Application

The minor system is comprised of stormwater network data acquired from the City and County of Denver Open Data Catalog including conduits, inlets, manholes, and underground storage as ArcGIS shapefiles. The delineated study area was used to isolate the portion of the stormwater network that contributes to flow to the downstream USGS gage. The stormwater network within the study area is comprised of 557 manholes, 508 inlets, and 9,272 km of conduits. The stormwater network drains to Harvard Gulch at multiple outlet locations distributed along the entire stream channel within the study area.

The open channel of Harvard Gulch was represented as a component of the minor system using irregular and open-trapezoid cross-sections. There are 27 bridge crossings of the Harvard Gulch channel within the study area; representation of the open channel as minor system conduits made it possible to easily represent the channel passing below the bridge decks (Matrix Design Group 2016). The irregular channel cross-sections were determined using the transect

tool in PCSWMM with the 1m DEM from the National Elevation Dataset resulting in 46 transects along the irregular channel. The trapezoidal channel was considered to be uniform with a maximum depth of 2.74 m, bottom width of 2.44 m, and top width of 9.75 m (Matrix Design Group 2016). Channel slopes were approximated from attributes of the conduits representing Harvard Gulch in the City and County of Denver stormwater data. Dry weather flows were computed from the streamflow recorded during the week prior to the simulation where no precipitation was recorded at the upstream USGS gage 06711570, and were applied as a constant inflow of 0.072 m^3/s at the closest irregular channel node to the upstream gage. The outfall of the minor system was assigned at the downstream USGS gage 06711575.

Subcatchments were delineated using the Voronoi decomposition tool in PCSWMM to create Theissen polygons based on the location of inlets in the watershed, resulting in 513 subcatchments. The average slope and percent imperviousness of the subcatchments were computed from the 3m DEM from the National Elevation Dataset to reduce local changes in elevation in the 1m DEM, and percent imperviousness was computed using the most recent impervious area data (2016) from the City and County of Denver, respectively (Table 1). The outlet of the subcatchments were assigned to be the lowest elevation 2D node (described below) adjacent to the minor system inlet used for subcatchment delineation. The assignment of the subcatchment outlet to a 2D node is recommended for modeling overland flow entering the minor system via inlets and to represent rainfall induced flooding. The rain gages located within the study area were assigned to subcatchments using Theissen polygons. The modified Green Ampt method was used to represent infiltration based on the soil classification of type C soil (Table 1).

2.2.2 Stormwater network data completeness

Although the stormwater network data available from the City and County of Denver is more complete than other municipalities in the region, there was still a considerable number of structures with unknown or incomplete details. Accurate structure details such as manhole and inlet inverts, conduit offsets, conduit geometry, inlet type, and storage node geometry are all important to the accuracy of a detailed stormwater model. Of the stormwater data available from the City and County of Denver for the study area, 78% of inlets, 28% of manholes, 6.6% of conduits, and 85% of surface and underground storage facilities were missing one or more important structure details..

In order to develop a minor system model that would accurately represent flow in the stormwater network, the missing stormwater structure data (e.g., manhole and inlet inverts, conduit slope, and conduit offsets) were approximated using a variety of methods, which are described in detail in Appendix A. In some cases, structure details were not unknown, but the method of recording stormwater network data in the City and County of Denver files differed from the way data is recorded in PCSWMM, which required extraction and restructuring of data from GIS layers prior to input to PCSWMM. There are only three underground storage nodes within the study area, two of which are underground detention pipes that were modeled using connected conduits and nodes. The third storage node was modeled as a rectangular detention vault with geometry determined from the area of the node feature in GIS and the depth attribute. Other surface storage within the study area could be included in the minor system as storage nodes; however, because the degree of missing or incomplete data available for the geometry of surface storage facilities, it was assumed that the surface storage is best represented in the major

system model by the topographical depressions in the DEM used to develop the major system model domain.

Table 1. Initial and calibrated PCSWMM parameters. Ranges are given for parameters which vary across subcatchments.

Parameter	Initial Value(s)	Calibration uncertainty	Calibrated value(s)	Data Source
Subcatchment area (km^2)	$2.0*10^4$ - 0.22	NA	No change	GIS area
Subcatchment slope (%)	0.04-1.82	25%	0.043-2.14	3m DEM
Subcatchment width (m)	1.02-1030.35	200%	1.28-2041.64	PCSWMM calculation
Impervious (%)	3.59-100	NA	No change	City and County of Denver
N-Impervious Roughness	0.012	20%	0.011	PCSWMM documentation
N-Pervious Roughness	0.15	NA	No change	PCSWMM documentation
Depression storage - impervious (mm)	1.9	20%	2.08	PCSWMM documentation
Depression storage - pervious (mm)	3.81	50%	3.12	PCSWMM documentation
% Zero Depression storage Impervious	25	NA	No change	PCSWMM default
% Routed to Pervious	6-97.5	NA	No change	Alley & Veenhuis (1983)
Suction head (cm)	22	NA	No change	SSURGO web soil survey (NRCS)
Conductivity (mm/hr)	0.15	50%	1.35	SSURGO web soil survey (NRCS)
Initial Deficit (fract.)	0.262	25%	0.237	SSURGO web soil survey (NRCS)

2.2.3 2D Major System Application

The 2D major system utilizes the same SWMM5 engine as in the 1D minor system to model overland flow by creating a mesh of links and nodes representing the surface of the study area. The depth of water is measured in the nodes, and dynamic wave routing is used to allow flow in connecting links, which are represented as wall-less rectangular conduits with a width of

the designated cell resolution. Input layers for the 2D major system application include road centerlines and widths, 1m DEM, and building outlines. All data sources were acquired from the City and County of Denver Open Data Catalog, apart from the 1m and 3m DEM, which were acquired from the National Elevation Dataset. To produce the 2D mesh, the study area was broken into separate bounding areas for roads and surrounding areas. Roads were assigned a rectangular mesh, cell resolution of 3.048 m (10 ft), and Manning's roughness of 0.14. The surrounding areas were assigned a hexagonal mesh with a 15.24 m (50 ft) cell resolution and Manning's roughness of 0.55. The total area delineated as roads was 0.70 km^2 and the surrounding area was 7.56 km^2. The PCSWMM documentation recommends that the maximum number of 2D cells in a model be around 100,000 cells. In order to remain near this limit and still capture detailed overland flow on the roadways, a much smaller resolution was used for the roadways than the surrounding area, as roadways are the area of interest for this study. The resulting 2D major system model consists of 125,420 nodes and 313,054 conduits, that delineate 126,153 2D cells. The 2016 building outline data from the City and County of Denver open data catalog was used as the obstructions layer, which excludes buildings from the 2D mesh.

2.2.4 Minor and Major System Connection

Interactions between the major and minor system domains occur primarily at inlet and outlet nodes. There are six known types of inlets within the study area that are described in the Transportation Standards and Details from the City and County of Denver Public Works Department that fall into three general categories: curb opening, grated, and combination. Inlets can be installed as multi-inlets with multiple openings in series capturing runoff at a single location (City and County of Denver Department of Public Works 2017). When runoff exceeds the inlet capacity or debris reduces the inlet capacity, runoff may pond around, pass over, or, in

more extreme cases, flow out of the inlet. Runoff re-enters the major system through outlets, most often conveying water into surface storage such as an extended detention basin, or into a stream channel. In more extreme storm events, interaction between the major and minor system can also occur due to surcharged manholes where the pressure of water in the manhole is great enough to lift the manhole cover and flow out of the minor system.

In PCSWMM, nodes in the minor system that represent inlets are connected to the major system nodes via outlets. When a minor and major system node is connected by an outlet, it is bidirectional, allowing water to flow in either direction into or out of the inlet depending on the elevation head of water in the inlet. Each connecting outlet is assigned a rating curve from City and County of Denver Storm Drainage Design and Technical Criteria based on the inlet type relating elevation head above the inlet to flow. There were 397 inlets within the study of an unknown type, and these were assigned an average rating curve (City and County of Denver Department of Public Works 2013). Minor system outlets to Harvard Gulch and surface storage facilities as well as the open channel conduits were connected to the major system with direct connections that co-locate the nearest major and minor system nodes. The invert elevation of 2D-nodes located within the stream channel were adjusted to match the bank-height of the channel in order to prevent double-counting the channel geometry in the 2D mesh and minor system conduit representing the channel.

2.3 Calibration and Validation

The model was calibrated using the Sensitivity-based Radio Tuning Calibration (SRTC) tool in PCSWMM. The SRTC tool varies parameters based on the parameter uncertainty (Table 1) (James 2003). Sensitivity analysis and calibration using the SRTC tool was performed for seven parameters: impervious Manning's roughness coefficient (n), pervious depression storage,

impervious depression storage, subcatchment slope, subcatchment width, soil hydraulic conductivity, and soil moisture initial deficit fraction.

The Mile High Flood District Stormwater Manual identifies the 80th percentile of storms that generate runoff in Denver, or about 15 mm of total rainfall, to be the optimal target storm event for GSI application (Mile High Flood District 2019). The simulation was run from 15:45 MDT to 23:45 MDT on June 24, 2015 during which a total rainfall of 20.07 mm fell. A storm of this size is between the 80th and 90th percentile of runoff causing storm events in Denver and exceeds the optimal target storm event by 5 mm (Mile High Flood District 2019). The primary precipitation event occurred between 16:55 MDT and 17:50 MDT and was followed by three small precipitation inputs of less than 2.54 mm over a 5 minute period. The storm event on June 24, 2015 was noted in the Matrix report for causing significant roadway flooding within Harvard Gulch (Matrix Design Group 2016). At a maximum intensity of 6.8 mm in 10 minutes, the storm does not exceed the Mile High Flood District criterion for roadway flood warnings of 0.5 in (12.7 mm) in 10 minutes, and would not have triggered automated warnings for roadway flooding. Nevertheless, the Matrix report described the event on June 24, 2015 as a storm that caused, “heavy flow in the streets when pipe capacity was exceeded…Residents noted 2.5 to 3 feet of water in their backyards, alleys, and streets” (Matrix Design Group 2016). There were seven dry days (no precipitation) recorded prior to the June 24th storm event. Outputs from the simulation were analyzed at a 5-minute time interval and calibrated to the streamflow recorded at the downstream USGS gage 06711575 for the length of the simulation. The calibrated model was validated by running a simulation for a precipitation event with a total of 8.6 mm and 10-min intensity of 3.56 mm on May 20, 2014 from 15:25 MDT to 16:05 MDT, which is less than the 75th percentile of all runoff causing storm events in Denver (Mile High Flood District 2019).

Model performance was assessed graphically and statistically. Statistics assessed include the coefficient of determination (R^2), Nash-Sutcliffe efficiency (NSE), root mean square error standard deviation ratio (RSR), and percent bias (%BIAS) (D. N. Moriasi et al. 2007). Additionally, there were 40 municipal service reports by residents to the Denver Department of Public Works between August 10, 2009 and November 25, 2019 of issues related to urban flooding, and two recurring flood locations in the study area, that were used to qualitatively validate the location of expected flooding in the study area due to this storm event. Although these reports do not provide specific details such as water depth on the roadway, they are useful for co-locating modeled surface flooding results with known locations of flooding.

2.4 GSI Scenario Application

The GSI scenarios were created by targeting 1%, 2.5%, 3.5% and 5% of the directly connected impervious area (DCIA) of each subcatchment for conversion to GSI. The method used for GSI application distributes the percent of impervious area treated evenly across all impervious area, rather than applying individual GSI units to specific locations. GSI units were represented by a bioretention cell with geometry and infiltration parameters (Table 2) for a streetside stormwater planter described in the City and County of Denver Ultra-Urban Green Infrastructure Guidelines (2016) (City and County of Denver 2016). No GSI were applied to subcatchments with less than 22.3 m^2 of DCIA (the surface area of a single bioretention cell), but the loss of treated area for these subcatchments was recovered by rounding up to the next whole number the number of bioretention cells applied to subcatchments with DCIA greater than 22.3 m^2. The amount of impervious area treated by each bioretention cell was approximated in the City and County of Denver Ultra-Urban Green Infrastructure Guidelines (2016) as 400 m^2 (City and County of Denver 2016). This area was used to determine what percentage of the

DCIA (minus the area converted to GSI) that was treated by the GSI scenario (Table 3). In the case that the area treated was larger than the subcatchment DCIA, the impervious area treated was limited to 100% of the DCIA, assuming that the disconnected impervious area was treated by surrounding pervious surfaces rather than GSI. Because the impervious area treated was limited to the DCIA within each subcatchment, the area treated by additional percentage of DCIA converted to GSI beyond 5% diminishes significantly.

Table 2. PCSWMM input parameters for a bioretention cell representing a streetside stormwater planter (GSI unit) from the City and County of Denver Ultra-Urban Green Infrastructure Guidelines (2016).

Layer	Parameter	Input Value
Surface	Berm height (cm)	20.32
	Surface roughness	0.1
	Surface slope (%)	1.0
Soil	Soil thickness (cm)	50.8
	Porosity (volume fraction)	0.453
	Field Capacity (volume fraction)	0.19
	Wilting point	0.085
	Conductivity (cm/hr)	1.1
	Suction head (cm)	11
Storage	Thickness (cm)	25.4
	Void ratio (voids/solids)	0.75
	Seepage rate (cm/hr)	0.25
	Clogging factor	0.1
Underdrain	Drain Coefficient (cm/hr)	222.5
	Drain exponent	0.5
	Drain offset height (cm)	0

Table 3. Values of the total study area converted to GSI, percent of impervious area converted to GSI, representative number of GSI units, and percent of impervious area treated for the four GSI scenarios.

GSI Scenario (DCIA converted)	Total Study Area Converted (km^2)	Impervious Area Converted (%)	GSI Units	Impervious Area Treated (%)
1%	0.014	0.34	566	5.9
2.5%	0.034	0.87	1572	16.6
3.5%	0.048	1.21	2213	23.5
5%	0.068	1.74	3178	33.2

CHAPTER 3 - RESULTS

3.1 Calibration and Validation

Sensitivity analysis of calibration parameters indicated that the most sensitive parameters were subcatchment slope, subcatchment width, and impervious Manning's coefficient; while pervious depression storage, hydraulic conductivity, initial deficit, and impervious depression were moderately sensitive parameters. The results of this sensitivity analysis are in agreement with previous studies of SWMM models (Panos et al. 2018; Rosa et al. 2015). The statistics computed comparing streamflow at the study area outfall (USGS gage 06711575) post-calibration indicates good model performance as described in Moriasi et al (2007) for all performance statistics with the exception of percent bias. The absolute value of percent bias greater than 25% indicates that the model was overpredicting the values of streamflow at the outfall, although the peak streamflow was underpredicted by 2.98 m^3/s (Figure 2). The validation simulation resulted in a significant reduction in model performance for prediction of streamflow at the study area outfall, suggesting that the calibrated model may not perform well for simulations of storms smaller than the calibration storm event (Table 4, Figure 2). Overprediction of streamflow for both the calibration and validation simulations was particularly notable for the falling limb of the hydrograph (Figure 2). Comparisons were made to streamflow as that is the only available quantitative data for comparison, although the model purpose was not to perfectly reproduce streamflow at the outfall but rather to represent roadway flooding within the model.

When the overall flood results (not isolating roadways) are compared with the recurring flood locations and resident reports, the reports were generally co-located with areas where

flooding is modeled (Figure 3). Areas where there is either a higher frequency of larger flood depths without co-location of resident reports or resident reports not co-located with flooding, are areas of concern for the general accuracy of the flood model. For example, located near where Harvard Gulch discharges into an underground rectangular conduit just upstream of the study area outfall, there was an area with depths approaching or exceeding 1m with no occurrence of co-located citizen reports. However, as reported in the Matrix report, depths of 2.5 to 3 feet (76 to 91 cm) were observed by citizens, which indicates that modeled depths within the upper range are not necessarily due to inaccuracies (Matrix Design Group 2016). The larger depths near the outfall may also be partially due to ponding of runoff at the boundary of the major system domain as there is no 2D flow exchange across the study area boundary. In the southwest of the study area there were five occurrences of resident reports related to flooding that were not co-located with modeled flooding, which indicate that the model may not be identifying flooding that occurs in this area or that the reports were made for a storm event with different spatial patterns of precipitation than the one modeled for this study.

Table 4. Performance statistics (coefficient of determination (R^2), Nash-Sutcliffe efficiency (NSE), root mean square error standard deviation ratio (RSR), and percent bias (%BIAS) for calibration and validation simulations of streamflow at the outfall.

Statistic	**Calibration**	**Validation**
R^2	0.849	0.516
RSR	0.0513	0.0643
NSE	0.745	0.422
%BIAS	-43.9%	-54.3%

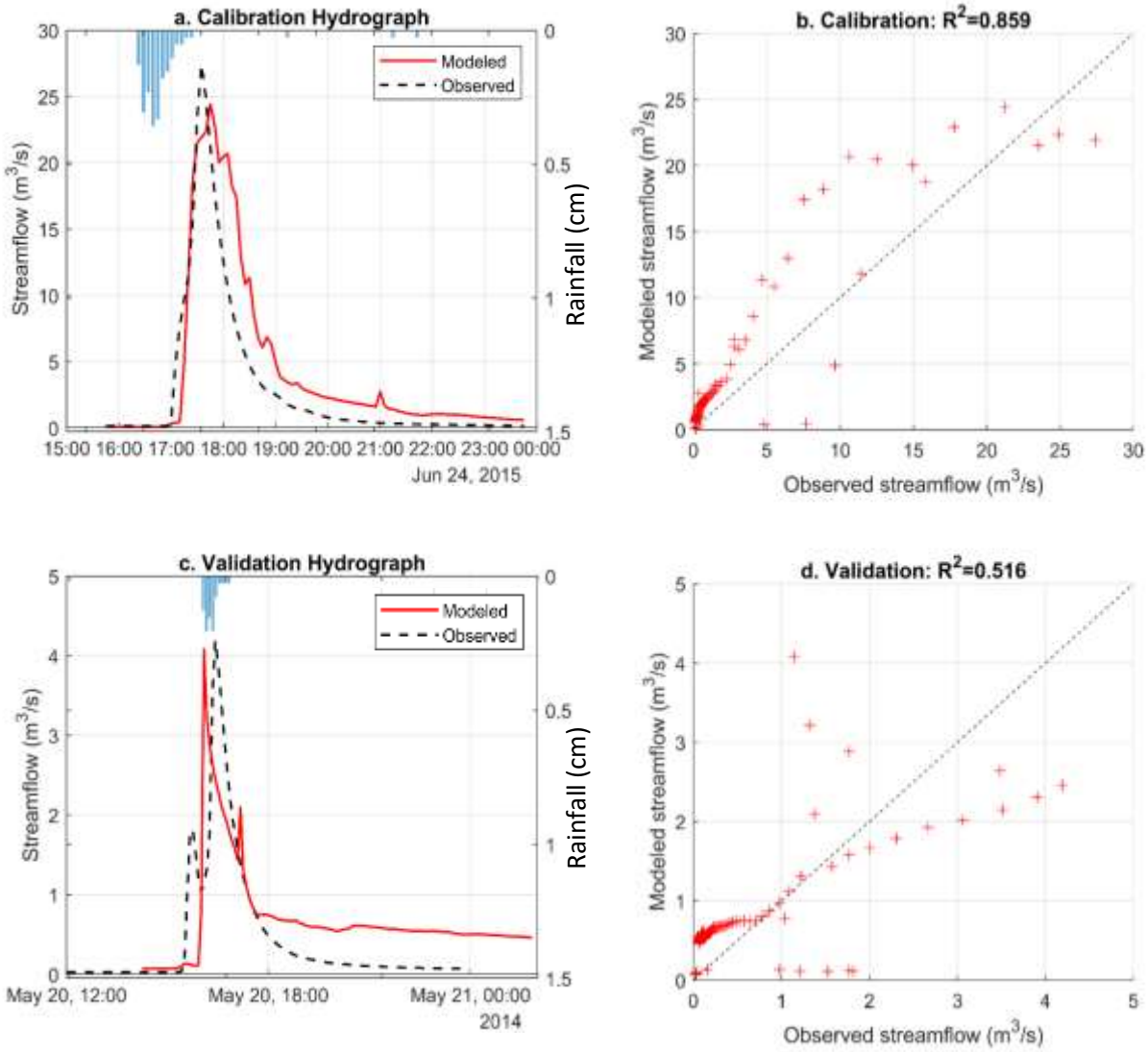

Figure 2. a. Modeled and observed streamflow at the study area outfall for the calibration simulation, b. modeled vs. observed streamflow for the calibration simulation, c. modeled and observed streamflow at the study area outfall for the validation simulation, and d. modeled vs. observed streamflow for the validation simulation. All data are reported at 5-minute intervals.

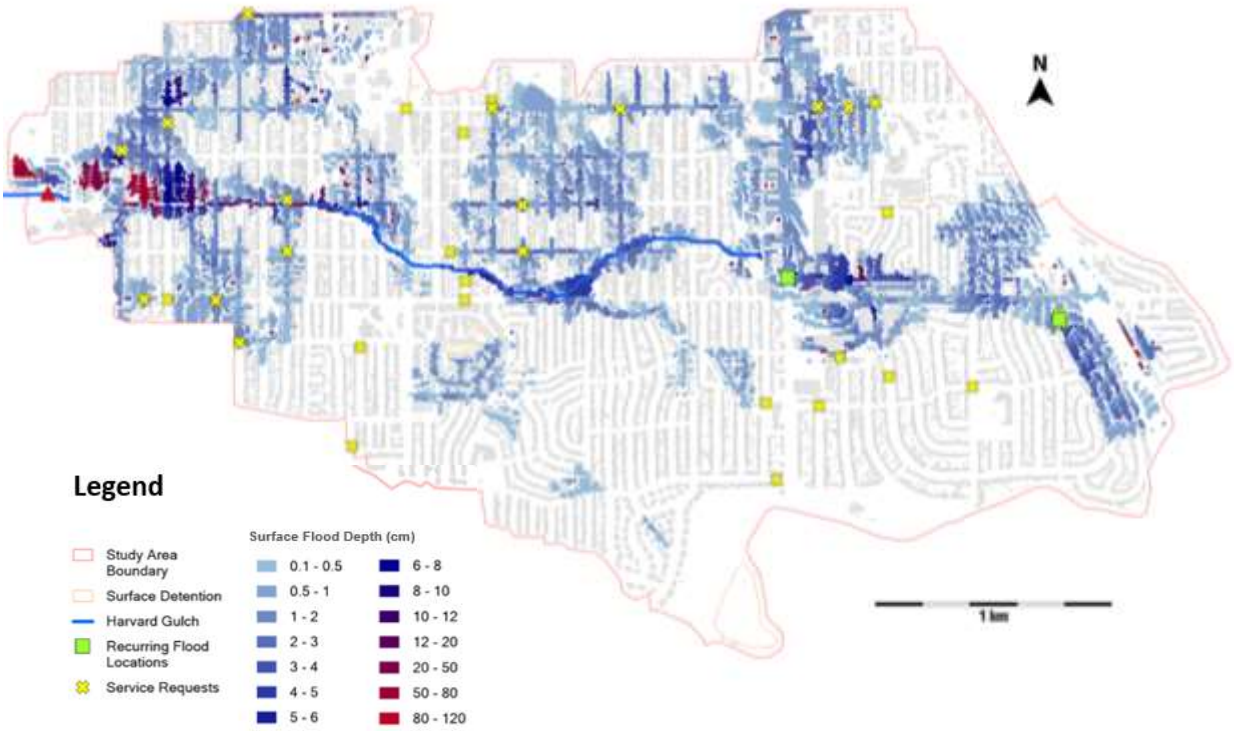

Figure 3. Overall flood extent and distribution of depths for the Pre GSI scenario during the peak flood extent at 18:30 MDT on June 24, 2015, with flood-related resident reports (service requests) from August 10, 2009 to November 25, 2019 made to the City and County of Denver Department of Public Works and DPW-identified recurring flood locations.

3.2 GSI Scenarios

The peak streamflow at the study area outfall was reduced for all GSI scenarios when compared to the Pre GSI scenario with a minimum percent reduction in peak streamflow of 2.56% for the 5% GSI scenario and maximum of 7.81% reduction for the 3.5% GSI scenario (Table 5, Figure 4). The time of the peak was not the same for all scenarios, but this may be due to numerical errors in the streamflow output near the peak as is suggested by the irregularly shaped peaks and by the smallest reduction of peak streamflow that occurred for the 5% GSI scenario (Table 5, Figure 4).

For all GSI scenarios, the spatial extent of roadway flooding was reduced for the entirety of the storm event, when compared to the baseline (Pre GSI) scenario (Figure 5). The reduction of roadway flood extent increased with percentage of DCIA converted to GSI, where the smallest reduction of roadway flood extent occurred in the 1% GSI scenario and the largest reduction occurred for the 5% GSI scenario for the entirety of the simulation (Figure 5). The roadway flood extent included the areas of 2D cells that overlay the roadway boundaries with water depths above the impervious depression storage depth of 0.208 cm; the flood depth was constant for the entire area of a 2D cell and the average 2D cell area representing the roadway is approximately 0.82 km^2. The roadway flood extent for all scenarios peaked at around 18:30 (Figure 5, Figure 6), 35 minutes following the end of the precipitation event (16:55-18:55), and between 35 to 55 minutes following the peak modeled streamflow depending on the GSI scenario (Table 5).

While the roadway flood extent changed similarly over time for the Pre GSI and GSI scenarios, there are slight differences in the rate at which the roadway flood extents increased to and receded from the peak extent (Figure 5). The roadway flood extent in the Pre GSI scenario increased and decreased faster than any of the GSI scenarios, at an average increase rate of 0.351 km^2/hr and decrease rate of 0.0212 km^2/hr. The slowest rates of increase and decrease in the GSI scenarios occurred for the 5% GSI scenario at 0.341 km^2/hr and 0.0203 km^2/hr, respectively. Despite having a faster rate of recession than the GSI scenarios, the Pre GSI scenario roadway flood extent was still larger than all GSI scenarios at the end of the simulation, indicating that the faster rate of recession did not overcome the increase in roadway flood extent reduction prior to the peak for the GSI scenarios. For each time shown in Figure 5, the 5% GSI scenario had the highest percent reduction of roadway flood extent and the 1% GSI scenario had the lowest

percent reduction compared to the other GSI scenarios, and for all scenarios the largest percent reduction occurred early in the storm, prior to the peak roadway flood extent at 18:30.

The mean flood depth for all scenarios peaked at 17:30 during the peak of the precipitation event, an hour earlier than the peak roadway flood extent (Figures 5 and 6). After 17:30, the mean flood depth for all scenarios decreased for the rest of the simulation, and the rate of the decrease slowed to nearly 0 cm/min as the average roadway flood depth approached 0 cm (Figure 6). Apart from 17:10, the percent reduction in roadway flood depth compared to the baseline scenario of the 5% GSI scenario was larger than that of the 2.5% GSI scenario. Between 18:30 and 20:30 the difference in percent reduction of mean roadway depth between the smaller GSI scenarios (1% and 2.5%) and the larger scenarios (3.5% and 5%) increased notably. However, after 20:30, the difference in percent reduction decreased to almost zero for all scenarios by the end of the simulation, indicating that below a threshold roadway flood depth around 1 cm, an increase in percent of DCIA converted to GSI is less ineffective. This result was further supported the distribution of roadway flood depths within the maximum roadway flood extent for the Pre GSI scenario at 17:30, when the peak mean roadway flood depth occurs (Figure 7). Although the peak mean flood depth (Figure 6) is around 4 cm for all scenarios at 17:30, the distribution of flood depth is not the same for all scenarios, with the 5% GSI scenario having the most cells with the shallowest flooding (Figure 7).

In addition to focusing on temporal variations within the storm, we also summed the difference of roadway flood extent between each GSI scenario and the Pre GSI scenario for each time shown in Figure 5 to give the total roadway flood extent reduction (km^2). The total roadway flood extent reduction was largest for the 5% GSI scenario (0.35 km^2 reduced), and smallest for the 1% GSI Scenario (0.066 km^2 reduced). However, when the total roadway flood extent

reduction was normalized by percent of DCIA converted to GSI in each scenario (i.e., the efficiency of roadway flood extent reduction), the most efficient scenario was the 2.5% GSI scenario with a total roadway flood reduction efficiency of 0.071 km^2 reduction per percentage of DCIA converted to GSI (Figure 8a). The least efficient scenario was the 1% GSI scenario with a total roadway flood reduction efficiency of 0.066 km^2 reduction per percentage of DCIA converted to GSI. Efficiency decreases slightly for the 3.5% and 5% GSI scenarios (Figure 8a) compared to the peak efficiency for the 2.5% GSI scenario.

This result is not replicated in the efficiency of reducing the mean roadway flood depth over the entire simulation (Figure 8b). To examine the efficiency of reducing the mean roadway flood depth, we summed the difference of mean roadway flood depth between each GSI scenario and the Pre GSI scenario for each time shown in Figure 5 to give the total mean roadway flood depth reduction (cm). The highest efficiency in reducing the mean roadway flood depth of 0.053 cm reduced per percentage of DCIA converted to GSI occurred for the 1% scenario, and the efficiency decreased as the percentage of DCIA converted increased, with the lowest efficiency of 0.028 cm per percentage of DCIA converted to GSI for the 5% GSI scenario.

To compare the spatial pattern within the watershed, we present a comparison of the differences in flood extents between two GSI scenarios (2.5% and 5%) among the roadway, non-roadway, and overall (roadway and non-roadway) areas (Figure 9). The non-roadway areas had the largest percent reduction for the entire 2.5% GSI scenario simulation, and the majority of the 5% GSI scenarios simulation compared to the overall area and roadway areas. The difference between the percent reduction of the non-roadway flood extent and the roadway flood extent was much less pronounced over the entirety of the simulation for the 5% GSI scenario. The largest percent reductions for all scenarios plotted occurred at the beginning of simulation. These

largest early reductions can also be seen in the extent and spatial distribution of depth of all flooding for a small area within the watershed for select times for the Pre and 5% GSI scenarios (Figure 10); the differences in spatial extent were much more pronounced at 17:30 than at 19:30.

The area shown in Figure 10 was of interest because of the multiple resident reports of flooding in the area and a location of recurring flooding identified by the City and County of Denver. These reports were co-located with larger flood depths that persist through 19:30 in both scenarios, indicating that the surface flood model was generally and qualitatively representing flooding patterns that would be expected for this area within the watershed. There was a clear difference in the flood extent and distribution of depths between the Pre and 5% GSI scenarios that occurs at 17:30, and the difference was especially pronounced in the NW portion of the inset. Additionally, the results shown in this area support the assumption made that the influence of existing surface storages within the watershed could be approximated using the elevation difference within the 2D surface model. The cells with the largest depths are co-located with the surface detention polygon located within this area of interest (Figure 10).

Table 5. Peak streamflow reduction (from Pre GSI) and peak streamflow timing for the four GSI scenarios in comparison to the Pre GSI scenario.

Scenario	**Peak (m^3/s)**	**Percent reduction (%)**	**Time of Peak**
Pre GSI	24.43	NA	17:45
1% GSI	22.93	6.15	17:55
2.5% GSI	22.92	6.16	17:35
3.5% GSI	22.52	7.81	17:40
5% GSI	23.8	2.56	17:35

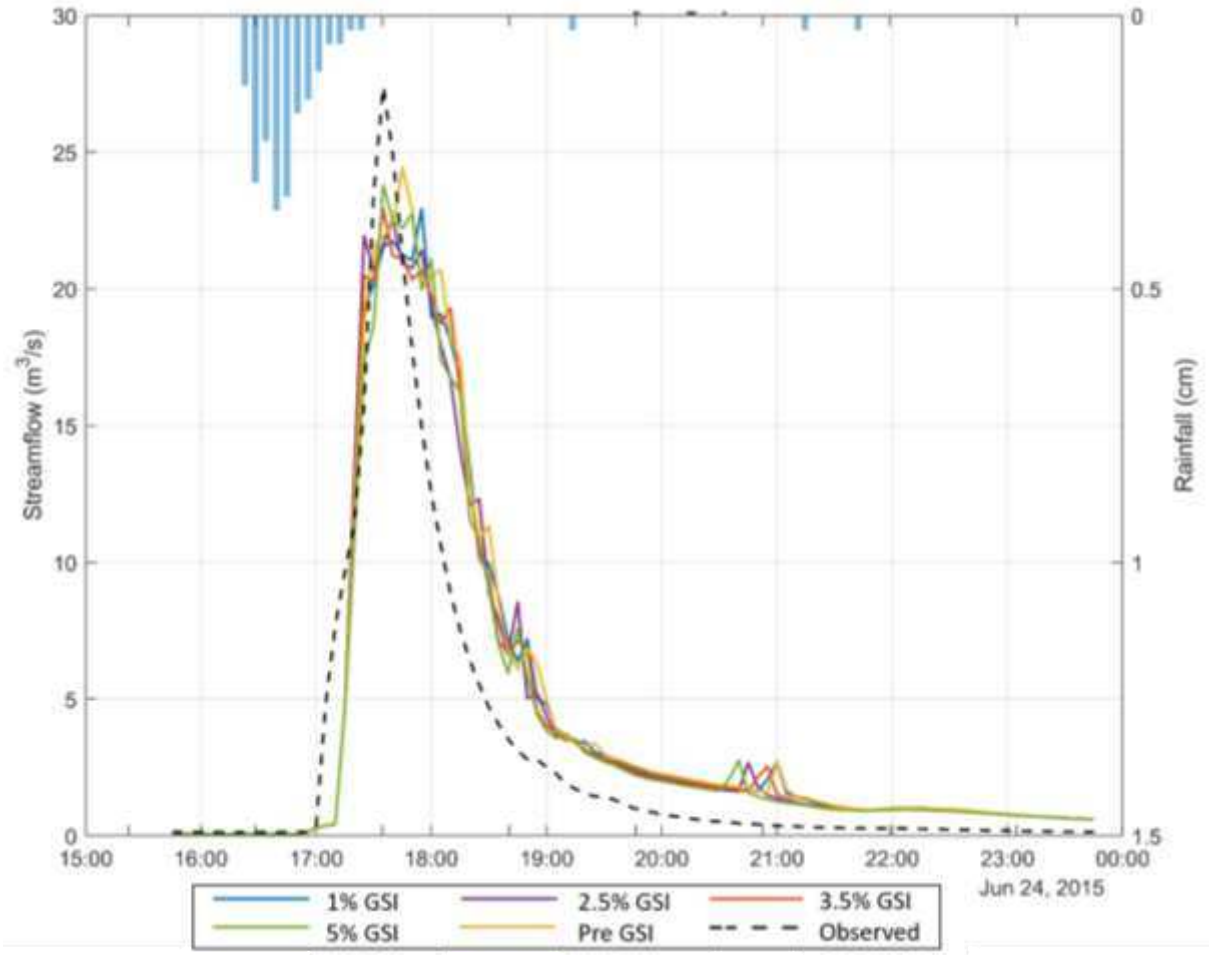

Figure 4. Observed, calibrated (Pre GSI), and modeled GSI scenario (1%, 2.5%, 3.5%, and 5%) streamflow at study area outfall with precipitation observed at USGS gage 393947104555101 at 5-minute time intervals.

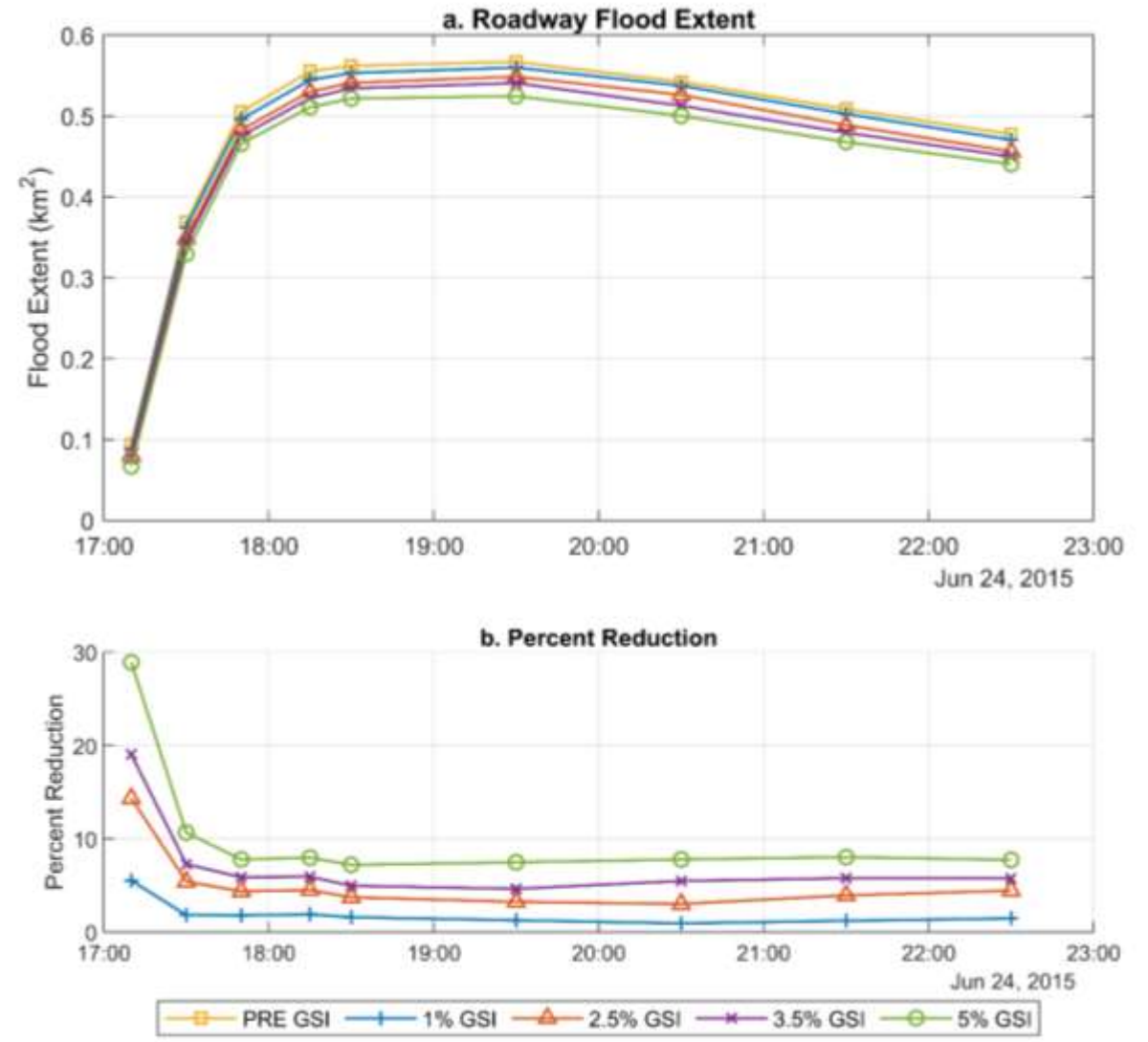

Figure 5. a. Roadway flood extent (km^2) at select times throughout the simulation period b. Percent reduction of roadway flood extent for GSI scenarios compared to the Pre GSI scenario.

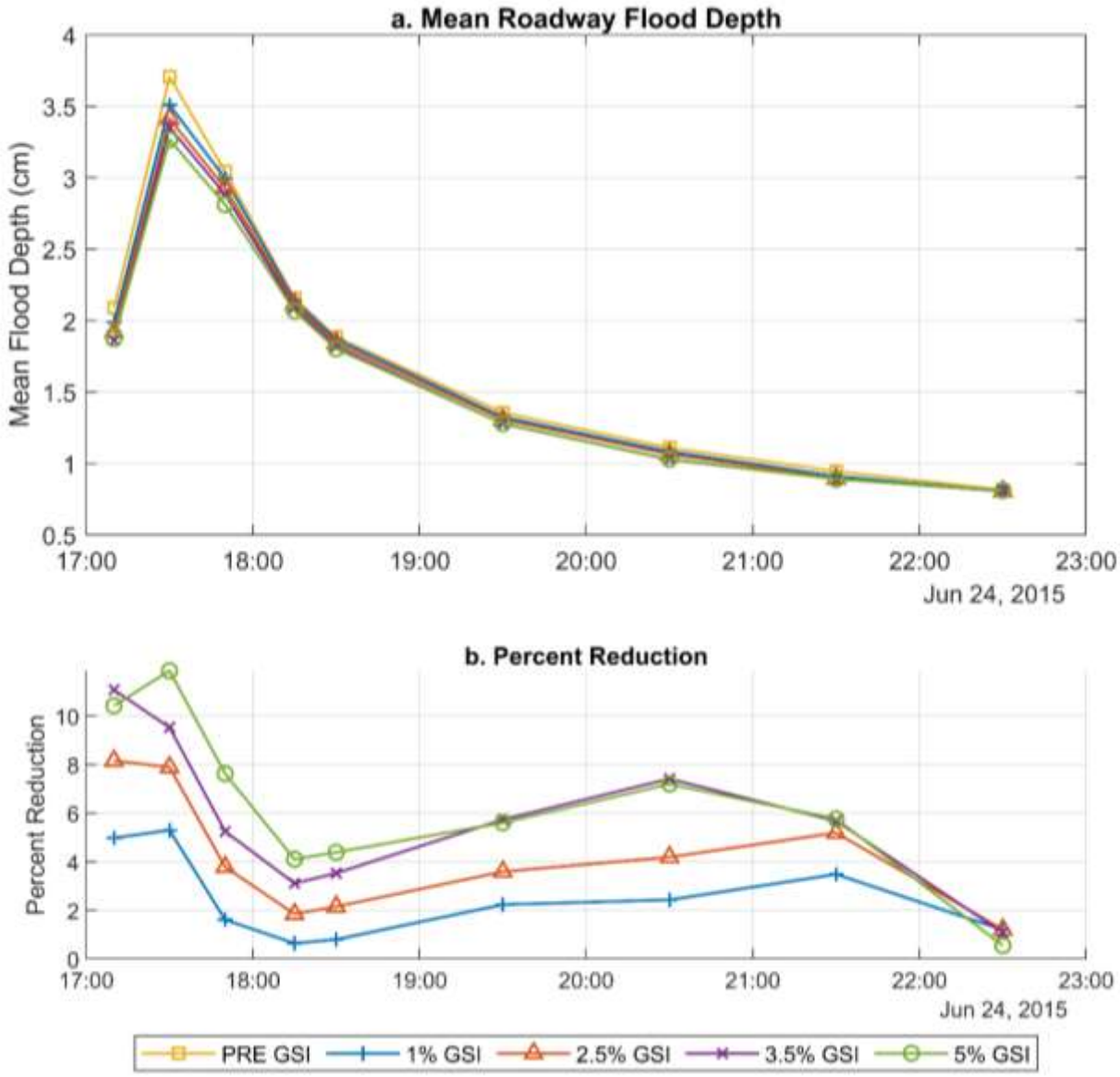

Figure 6. a. Mean roadway flood depth (cm) at select times throughout the simulation period b. Percent reduction of mean roadway flood depth for GSI scenarios compared to the Pre GSI scenario.

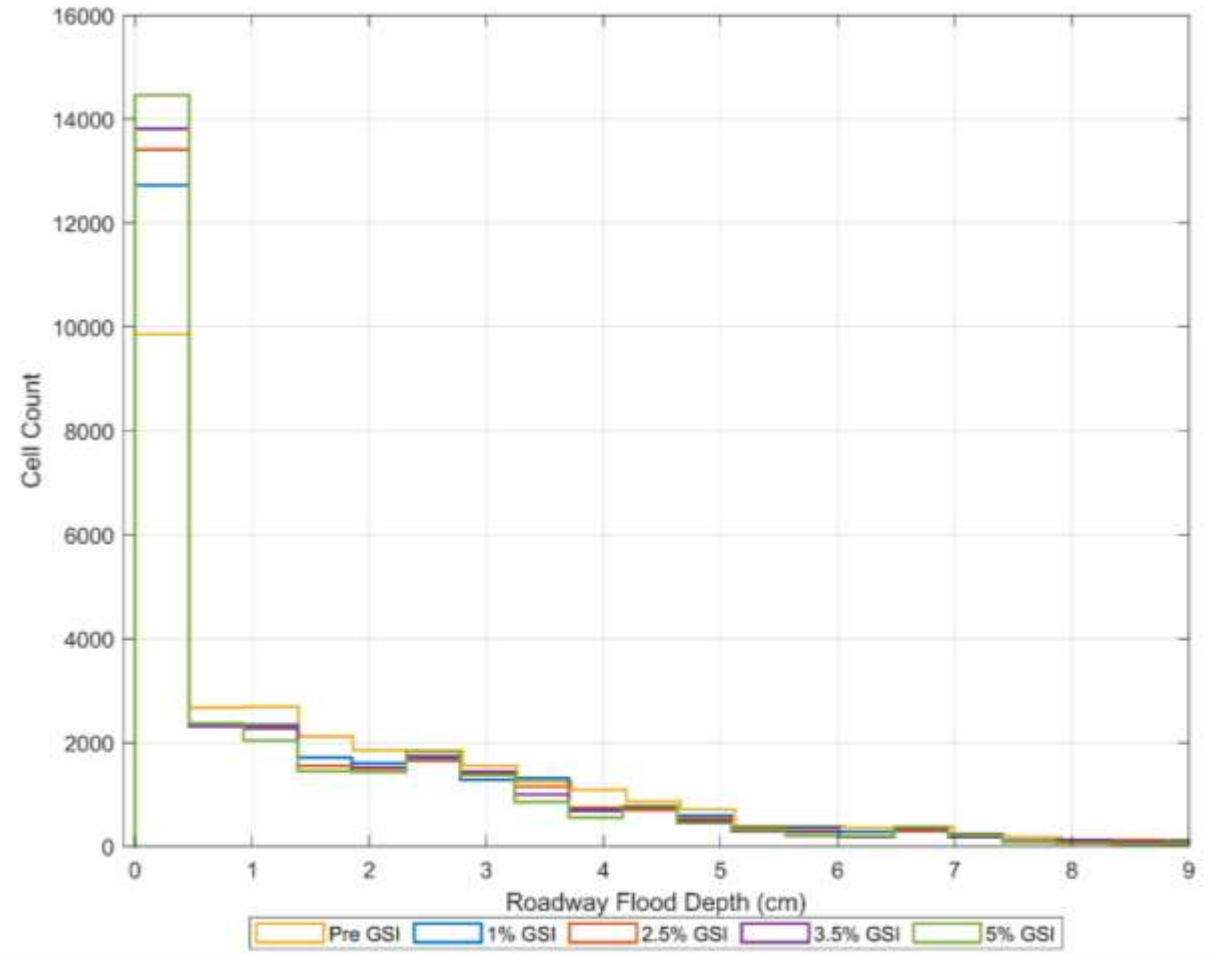

Figure 7. Histogram of roadway flood depth distribution across model cells at 17:30 on June 24, 2015. The number of cells plotted is the maximum cell count that has roadway flooding (33,295 cells) from the Pre GSI scenario at 18:30 for all histograms. The roadway flood depth axis is limited to a maximum of 9 cm; less than 2% of 2D cells have flood depths above 9 cm.

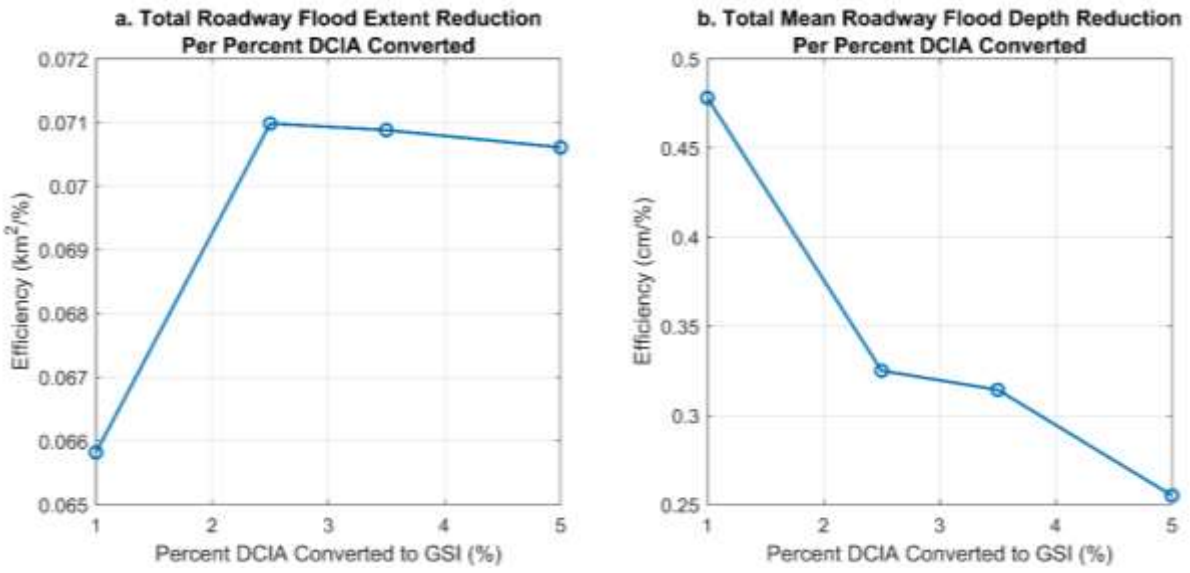

Figure 8. a. Total roadway flood extent reduction over the duration of the simulation (km^2) normalized by the percentage of DCIA converted to GSI vs. percent DCIA converted to GSI, b. Total mean roadway flood depth reduction over the duration of the simulation (cm) normalized by percentage of DCIA converted to GSI vs. percent DCIA converted to GSI.

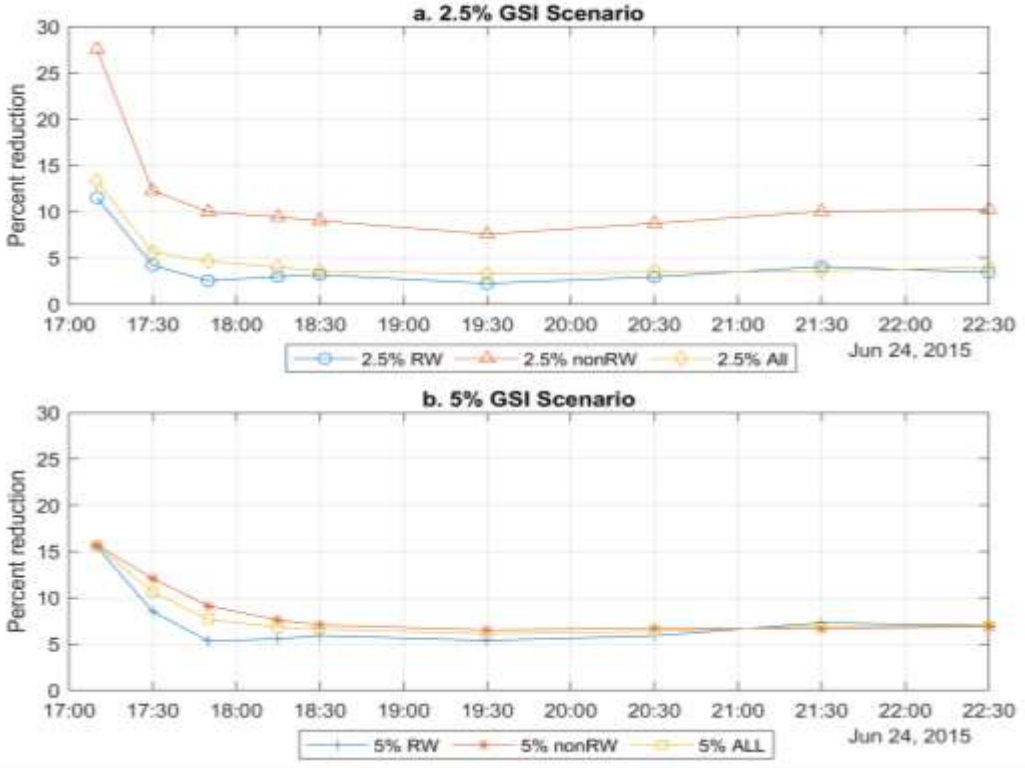

Figure 9. Percent reduction of roadway (RW), non-roadway (nonRW), and combined flood extent (ALL) compared to the Pre GSI scenario for (a) 2.5% GSI conversion and (b) 5% GSI conversion.

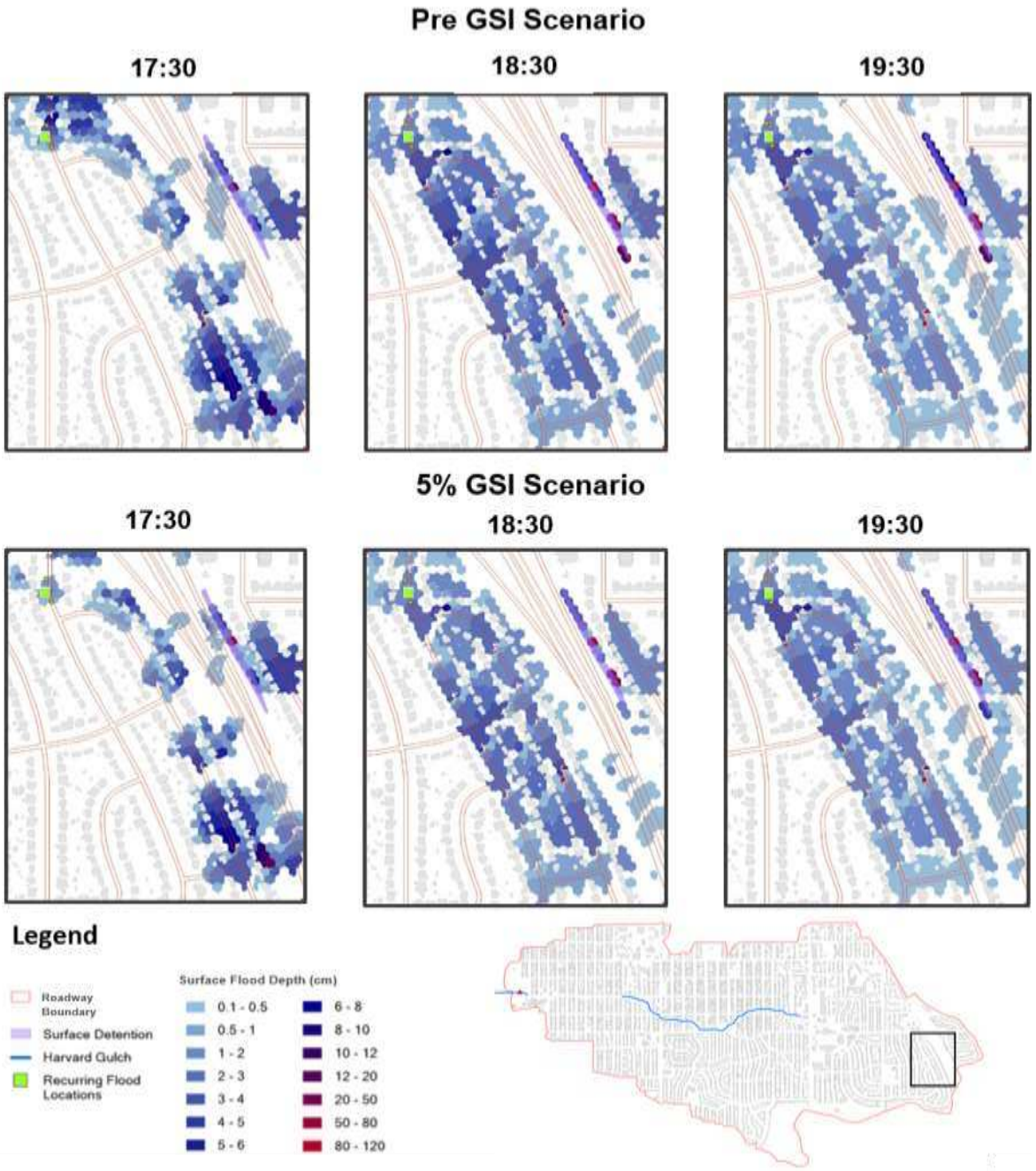

Figure 10. The surface flood extent and depth for a small portion (0.02 km^2) of the watershed at select times for the Pre and 5% GSI scenarios.

CHAPTER 4 - DISCUSSION

The results described above indicated that the conversion of even 1% of the DCIA to GSI lead to the reduction of mean roadway flood depth and spatial extent, and increasing the amount of GSI added to 5% of the DCIA further reduced the mean roadway flood depth and spatial extent (Figures 5 and 6). Previous studies examining impacts of GSI on urban flood depths at stormwater nodes found that the minimum percentage of DCIA converted to GSI necessary to observe an impact was between 5% and 20% converted (Palla and Gnecco 2015; Walsh et al. 2014; Zellner et al. 2016). The reduction seen in this study at 1% DCIA converted to GSI suggests that, although the other studies examined different watersheds, storms, and modeling procedures, modeling urban flooding as a 2D surface may be more sensitive to the addition of GSI than when floods are only examined at stormwater nodes. Additionally, the variation in the distribution of depths for the GSI scenarios (Figure 7) indicates that examining the distribution of depths rather than the mean depth may provide further insight into the effects of GSI on roadway flooding.

The difference in percent reduction of both roadway flood extent and mean depth were not constant over the entirety of the simulation (Figures 5 and 6). For both reduction measures, the difference in percent reduction between the GSI scenarios was most pronounced in the first 20-40 minutes of the simulation results, smallest around the peak, and then increased slowly for the remainder of the simulation. Increasing the percentage of DCIA converted to GSI had the largest effect during the precipitation event, but the effects were less pronounced as the flood extent and mean depth approached their peak values (Figures 5b and 6b). The effect of GSI on percent reduction of flood extent and mean depth then increased again as the flooding recedes,

but never regained the percent reduction seen at the beginning of the simulation. By comparing the efficiency of roadway flood extent per percent DCIA converted to GSI for the GSI scenarios, we observe a maximum efficiency at 2.5% of DCIA converted to GSI and a diminished return for greater conversion. In contrast, for the efficiency of mean roadway flood depth reduction, the maximum efficiency was observed at 1% of DCIA conversion to GSI (Figure 8). This indicates that flood metrics of depth and extent differ in their response to the addition of GSI, although in both cases additional GSI conversion beyond 2.5% of DCIA yielded diminished returns.

The larger percent reduction of non-roadway flood extents (Figure 9) may be explained by the method used to add GSI to the subcatchments within the model. In the models developed for this study, the GSI were not spatially represented. Instead, the effects of the GSI were distributed evenly throughout the impervious area of the subcatchment. The roadway flood results for the GSI scenarios were influenced by local elevation changes, surface roughness of roadways, and location of stormwater inlets near roadways; but the percent reduction of spatial extent and flood depth on the roadway cannot be attributed to the specific placement of GSI.

Although there are methods available in PCSWMM that allow for the spatial application of GSI by creating individual subcatchments for each GSI unit, this methodology is not conducive to the addition of large numbers of GSI to the model. In this study, between 566 and 3,158 GSI units were added to the1% and 5% GSI scenarios, respectively, which exceeds a reasonable number of GSI units to utilize the methodology for spatial placement. To use the spatial representation of GSI as individual subcatchments, the placement and parameter assignment for each individual GSI must be performed manually, and the development of multiple scenarios requires manual edits for each GSI. There is little opportunity for automating the addition or editing of GSIs within PCSWMM. In addition to the high labor demand of

implementing spatial GSI, the addition of over 500 GSI represented as relatively small $22.3*10^{-5}$ km^2 subcatchments (whereas the average area of subcatchments within the model is $16.1*10^{-3}$ km^2), would lead to an even greater computational demand that may be time prohibitive. For example, when run individually, each scenario took 17-20 hours to complete when run on 12 CPUs, and these simulations did not represent GSI as individual subcatchments. Run times may be further increased because the implementation of small GSI subcatchments may require a finer routing time-step to achieve reasonable model routing errors. The impact of not modeling the specific locations of GSI on the accuracy of results of 2D surface flood has not been established by the current body of research, but has been noted as a limitation in previous studies (Elliott and Trowsdale 2007).

A significant challenge influencing the reliability of the simulation results is the short (single event) calibration simulation and the lack of data available to calibrate the 2D surface flooding component of the model. The only available data for calibration within the study area is streamflow at the USGS outlet gage, therefore to develop a model that could be calibrated using USGS streamflow data at the watershed outlet, the study area had to include all area that would drain via surface runoff and the stormwater network to the stream channel at the USGS gage. Often, stormwater models are calibrated using long-term simulations with multiple storm events of varying characteristics, including the interaction between antecedent conditions of successive storm events with runoff. However, because of the long simulation times and computational demand of the model used in this study, calibration simulation run times for a limited number of parameters (Table 1) for a single storm event exceeded 60 hours. In order to calibrate for a continuous precipitation record containing multiple storms, a larger computational capacity would have been required. The model calibration for streamflow resulted in calibration statistics

that are characteristic of a "good" model (D. N. Moriasi et al. 2007) (Table 4). When the model was tested for a validation storm that has a total rainfall that is 12.1 mm smaller than the storm used as the calibration event, the quality of the modeled streamflow compared to observed data deteriorated considerably (Table 4). This indicates that although the model was well-calibrated for the storm event used to simulate all three scenarios, the transferability of the model to other storm events is poor.

In addition to challenges calibrating the dual drainage model with available streamflow data, the complete absence of quantitative roadway flood depth data does not allow for a test of the reliability of modeled roadway flooding depth results. The method used to model flooding in this study results in detailed local flood extent and depth results (Figure 10), but without accurate observations of flooding localized variations cannot be verified. A potential solution to the lack of urban flood observation data is the utilization of resident (311) reports of flooding and known recurring flood locations defined by the City and County of Denver. These reports rarely contain quantitative information on depth or distribution of flooding and therefore the utility in validation is limited to co-location with modeled flooding (Figures 3 and 10). Additionally, the number and distribution of reports pertaining to a single storm event is not large enough to validate flood data within an entire watershed. This is an issue particularly for validating roadway flooding that falls within the category of nuisance flooding because the water surface may be below the depth that would incline residents to file a 311 report.

Other limitations are related to stormwater input data and representation. Despite the effort made to utilize the most accurate and relevant information to fill in missing stormwater structure details, the approximation of structure geometry and parameters introduced uncertainty to the model outputs that cannot be quantified or overcome by calibration of the 2D flood model.

Furthermore, the accuracy of 1D-2D exchange between surface runoff and the stormwater network modeled using orifice-based equations (in this study a rating curve based on the orifice relationship is used) has been questioned. A study performed by Bazin Pierre-Henri et al. (2014) concluded that a numerical exchange model rather than an orifice relationship was necessary to accurately model experimental data for a scale model with a single inlet. This further emphasizes the need for more urban flood calibration data to overcome the potential error in the physical representation of how water is exchanged between the surface and subsurface networks.

In order to improve the accuracy of this type of model for the full range of storm event sizes, larger computational capacity would be needed to calibrate the model for a continuous, longer term precipitation record. Crowdsourced science and/or resident reports to municipalities have the potential to increase the quantity of observations of urban flooding, as seen in Smith and Rodriguez (2017). However, a large-scale campaign to encourage resident reporting of flooding, as well as education on what characterizes a roadway flood in order to capture nuisance-size flood depths, would be needed to collect a large enough quantity of data capturing the entire range of urban flood event depths. An ongoing project at CSU developed an application called FloodTracker that allows residents to report geo-tagged and categorically quantitative urban flood data to address the need for urban flood data and utilize crowdsourced science ("Flood Tracker.org" n.d.). The quantification of how 2D roadway flooding data influences traffic systems has not yet been established. Previously, Hou et al. (2017) used microscopic traffic flow simulations to assess the accident vulnerability of vehicles during hazardous driving conditions, and future work will benefit from examining how specific hazardous driving conditions such as roadway flooding impact vehicle safety.

To gather a more detailed understanding of how GSI placement affects roadway flooding, the ability to automate placement and parameter assignment for representative GSI subcatchments within PCSWMM as an input data file would greatly improve the efficiency of modeling spatially representative GSI units, and further study will be needed to assess the impact of modeling GSI with dual drainage at both the watershed and site-scales. Additionally, there is a discrepancy in the studies that have examined theoretical GSI network effects on urban flooding (Pregnolato et al. 2016; Qin et al. 2013; Zhu and Chen 2017) and the study of how realistic GSI network scenarios based on municipality practices future plans affect urban flooding. However, before embarking on further development of complex dual drainage models, the fundamental challenge of complete and accurate input data including stormwater network data, soil data, and precipitation data is necessary.

CHAPTER 5 - CONCLUSIONS

Modeling stormwater structure-scale interaction between green stormwater infrastructure (GSI), surface runoff, and stormwater networks to examine the extent, depth, and distribution of 2D roadway flooding within a watershed is critical to expand the understanding of how GSI impact urban systems such as transportation networks. With a detailed dual drainage model of Harvard Gulch, Denver, Colorado and GSI scenarios applied as a percentage of the directly-connected impervious area (DCIA) converted to bioretention cells, it was shown that even at 1% of the DCIA converted to GSI, there was a decrease in the extent and mean depth of roadway flooding, as well as localized changes to flood extent and distribution of depths. This study provides an example of a watershed-scale, detailed dual drainage model and identifies challenges that can be used to direct future work on the structure-scale interaction between GSI, stormwater structures, and 2D surface runoff.

How can 1D-2D dual drainage modeling help determine the effect of GSI networks on the depth, flooded extent, and spatial distribution of roadway flooding?

- The modeled streamflow results show that for this specific storm event, the dual drainage model can provide realistic streamflow outputs (Figure 2), which for a model without a 2D flood domain, would indicate acceptable model performance (Table 4).
- With an understanding of the reliability of results, the major system flood model was able to show that the conversion of only 1% DCIA to GSI reduced the spatial extent (Figure 5) and mean depth (Figure 6) of roadway flooding, particularly during the beginning and end of the storm response.

- Conversion of increasing percentages of DCIA to GSI (1%, 2.5%, 3.5%, and 5%) further reduced the flood spatial extent and flood mean depth (Figures 5 and 6), although with diminishing returns (Figure 8).
- Results of the major system flood model show localized variation in flooding that indicate the value of a dual drainage model in understanding the structure-scale interactions between GSI, stormwater structures, and runoff, given that these results could be verified by observation of urban flooding (Figures 3 and 10).

What are the limitations of dual drainage 1D-2D modeling for characterizing the effects of GSI networks on roadway flooding?

- The model developed lacks spatially-specific GSI network implementation as the model methods to represent GSIs in space were not scalable to large watersheds. Future work to improve incorporation of spatially-specific GSIs efficiently into stormwater models will clarify the importance of this challenge.
- Although we knew that the specific storm event modeled produced roadway flooding, there was still not spatially-distributed data on the depth and timing of roadway flooding that could be used to compare to modeled roadway flooding model results. Crowdsourced science and resident reporting have the potential to provide critically needed calibration data for urban flooding, but a significant increase in the quantity and distribution of these reports is needed.
- Additional computational capacity is needed to calibrate a 1D-2D dual drainage model of this size and complexity using a continuous long-term precipitation and streamflow record.

There is potential that, with the continued improvement of modeling techniques and technology as well as efforts to improve input and calibration data, development of detailed watershed scale dual drainage models can address gaps in the understanding of structure-scale interactions over the entirety of a study watershed.

REFERENCES

Alley, W. M., and Veenhuis, J. E. (1983). "Effective Impervious Area in Urban Runoff Modeling." *Journal of Hydraulic Engineering*, 109(2), 313–319.

Askarizadeh, A., Rippy, M. A., Fletcher, T. D., Feldman, D., Peng, J., Bowler, P., Mehring, A., Winfrey, B., Vrugt, J., AghaKouchak, A., Jiang, S., Sanders, B. F., Levin, L. A., Taylor, S., and Grant, S. B. (2015). "From rain tanks to catchments: Use of low-impact development to address hydrologic symptoms of the urban stream syndrome." *Environmental Science & Technology*.

Bazin Pierre-Henri, Nakagawa Hajime, Kawaike Kenji, Paquier André, and Mignot Emmanuel. (2014). "Modeling Flow Exchanges between a Street and an Underground Drainage Pipe during Urban Floods." *Journal of Hydraulic Engineering*, 140(10), 04014051.

CHI Water. (n.d.). "Computational Hydraulics International (CHI)." <https://www.chiwater.com/Home> (Jun. 19, 2020).

City and County of Denver. (2015). "Denver Open Data Catalog." <https://www.denvergov.org/opendata/> (Jun. 19, 2020).

City and County of Denver. (2016). "Ultra-Urban Green Infrastructure Guidelines." <https://www.denvergov.org/content/denvergov/en/wastewater-management/stormwater-quality/ultra-urban-green-infrastructure.html> (Jun. 19, 2020).

City and County of Denver. (2018). "Green Infrastructure Implementation Strategy." <https://www.denvergov.org/content/denvergov/en/wastewater-management/stormwater-quality/green-infrastructure/implementation.html> (Jun. 19, 2020).

City and County of Denver Department of Public Works. (2013). *City and County of Denver Storm Drainage Design and Technical Criteria*.

City and County of Denver Department of Public Works. (2017). *Transportation Standards and Details for the Engineering Division*.

D. N. Moriasi, J. G. Arnold, M. W. Van Liew, R. L. Bingner, R. D. Harmel, and T. L. Veith. (2007). "Model Evaluation Guidelines for Systematic Quantification of Accuracy in Watershed Simulations." *Transactions of the ASABE*, 50(3), 885–900.

Djordjević, S., Prodanović, D., and Maksimović, Č. (1999). "An approach to simulation of dual drainage." *Water Science and Technology*, 39(9), 95–103.

Elliott, A. H., and Trowsdale, S. A. (2007). "A review of models for low impact urban stormwater drainage." *Environmental Modelling & Software*, 22(3), 394–405.

Field, C. B., Barros, V., Stocker, T. F., and Dahe, Q. (Eds.). (2012). *Managing the Risks of Extreme Events and Disasters to Advance Climate Change Adaptation: Special Report of the Intergovernmental Panel on Climate Change*. Cambridge University Press, Cambridge.

"Flood Tracker.org." (n.d.). <https://floodtracker.org/> (Jun. 19, 2020).

Galloway, G. E., Reilly, A., Ryoo, S., Riley, A., Haslam, M., Brody, S., Highfield, W., Gunn, J., Rainey, J., and Parker, S. (2018). "The Growing Threat of Urban Flooding: A National Challenge." *College Park and Galveston: University of Maryland and Texas A&M University*.

Hou, G., Chen, S., Zhou, Y., and Wu, J. (2017). "Framework of microscopic traffic flow simulation on highway infrastructure system under hazardous driving conditions." *Sustainable and Resilient Infrastructure*, 2(3), 136–152.

Jacobs, J. M., Cattaneo, L. R., Sweet, W., and Mansfield, T. (2018). "Recent and Future Outlooks for Nuisance Flooding Impacts on Roadways on the U.S. East Coast." *Transportation Research Record: Journal of the Transportation Research Board*, 2672(2), 1–10.

James, W. (2003). *Rules for responsible modeling*. CHI, Guelph, Ont.

Jefferson, A. J., Bhaskar, A. S., Hopkins, K. G., Fanelli, R., Avellaneda, P. M., and McMillan, S. K. (2017). "Stormwater management network effectiveness and implications for urban watershed function: A critical review." *Hydrological Processes*, 31(23), 4056–4080.

Lee, J. G., Selvakumar, A., Alvi, K., Riverson, J., Zhen, J. X., Shoemaker, L., and Lai, F. (2012). "A watershed-scale design optimization model for stormwater best management practices." *Environmental Modelling & Software*, 37, 6–18.

Liwanag, F., Mostrales, D. S., Ignacio, Ma. T. T., and Orejudos, J. N. (2018). "Flood Modeling Using GIS and PCSWMM." *Engineering Journal*, 22(3), 279–289.

Matrix Design Group. (2016). *Harvard Gulch and Dry Gulch Major Drainageway Plan: Conceptual Design Report*. Design, Denver, CO.

Mile High Flood District. (2019). "Criteria Manual Volume 3." *Mile High Flood District*, <https://mhfd.org/resources/criteria-manual-volume-3/> (Jul. 7, 2020).

NOAA. (n.d.). "Climate at a Glance | National Centers for Environmental Information (NCEI)." <https://www.ncdc.noaa.gov/cag/county/mapping/5/pcp/201911/12/value> (Jun. 19, 2020).

Palla, A., and Gnecco, I. (2015). "Hydrologic modeling of Low Impact Development systems at the urban catchment scale." *Journal of Hydrology*, 528, 361–368.

Panos, P. C., Hogue, T. S., Gilliom, R., and McCray, J. (2018). “High-Resolution Modeling of Infill Development Impact on Stormwater Dynamics in Denver, Colorado.” *Journal of Sustainable Water in the Built Environment*, 4(4), 04018009.

Perez-Pedini, C., Limbrunner, J., and Vogel, R. (2005). “Optimal Location of Infiltration-Based Best Management Practices for Storm Water Management.” *Journal of Water Resources Planning and Management*, 131(6), 441–448.

Pregnolato, M., Ford, A., and Dawson, R. (2016). “Disruption and adaptation of urban transport networks from flooding.” *E3S Web of Conferences*, (M. Lang, F. Klijn, and P. Samuels, eds.), 7, 07006.

Qin, H., Li, Z., and Fu, G. (2013). “The effects of low impact development on urban flooding under different rainfall characteristics.” *Journal of Environmental Management*, 129, 577–585.

Rosa, D. J., Clausen, J. C., and Dietz, M. E. (2015). “Calibration and Verification of SWMM for Low Impact Development.” *JAWRA Journal of the American Water Resources Association*, 51(3), 746–757.

Schmitt, T., Thomas, M., and Ettrich, N. (2004). “Analysis and modeling of flooding in urban drainage systems.” *Journal of Hydrology*, 299(3–4), 300–311.

Shuster, W. D., Bonta, J., Thurston, H., Warnemuende, E., and Smith, D. R. (2005). “Impacts of impervious surface on watershed hydrology: A review.” *Urban Water Journal*, 2(4), 263–275.

Smith, B. K., and Rodriguez, S. (2017). “Spatial Analysis of High-Resolution Radar Rainfall and Citizen-Reported Flash Flood Data in Ultra-Urban New York City.” *Water*, 9(10), 736.

Urbonas, B., Jansekok, M., and Guo, J. C. Y. (1990). *Effect of Raingage Density on Runoff Simulation Modeling*.

Walsh, T. C., Pomeroy, C. A., and Burian, S. J. (2014). “Hydrologic modeling analysis of a passive, residential rainwater harvesting program in an urbanized, semi-arid watershed.” *Journal of Hydrology*, 508, 240–253.

Zellner, M., Massey, D., Minor, E., and Gonzalez-Meler, M. (2016). “Exploring the effects of green infrastructure placement on neighborhood-level flooding via spatially explicit simulations.” *Computers, Environment and Urban Systems*, 59, 116–128.

Zhu, Z., and Chen, X. (2017). “Evaluating the Effects of Low Impact Development Practices on Urban Flooding under Different Rainfall Intensities.” *Water*, 9(7), 548.

APPENDIX A

The large proportion of stormwater structures with incomplete or missing structure details required the development of a process to fill or correct structure details using the most relevant known information about the individual and surrounding structures. The goal of this process was to maximize the accuracy of structure-specific input data for the stormwater network. Along with the process for filling and correction structure details, assumptions made in determining input values are described below:

1. If a junction is missing attribute data, the value may be recorded in one of the connected conduits.
    a. The junction invert attribute entered in PCSWMM was the lowest invert of the connected conduits; it was assumed that the invert of the lowest conduit has a zero offset.
2. If a junction is missing invert details:
    a. If connected conduits have invert data, use the lowest connected conduit invert
    b. If connected conduits do not have invert data,
        i. Use length and slope attributes from connected conduits and known junction invert to compute
        ii. If connected conduits have missing slope attribute
            1. For inlets,
                a. If inlet type is known, use default inlet depth based on inlet type from the city and county of Denver standard specifications

b. If inlet type is unknown, use default connected conduit slope of 2% (based on Denver standard specification)

2. For manholes, assume nearest known slope is continuous and extrapolate from nearest known junction attribute

c. Some junctions in the stormwater network data represent a pipe-to-pipe connection. The invert of these is interpolated from the nearest known junction invert using the conduit slope

3. If the ground elevation of an inlet or manhole is unknown use the 1m DEM elevation
4. Conduit offsets were computed from the difference between known conduit inverts and junction inverts.
    a. If only the upstream or downstream conduit invert was known, the missing invert was computed using the slope and length, and then the offset was computed.
    b. If neither upstream or downstream conduit inverts or the slope were known, the offset was assumed to be zero.
    c. If a zero offset resulted in a negative conduit slope, the slope was assumed to be the same as a neighboring in-line conduit and the offset was recomputed.
5. If conduit geometry is unknown, it was assumed to be the same as the nearest known conduit geometry.

To complete the minor system, the stormwater network was audited using tools available in PCSWMM. Orphans, stormwater structures that are not connected to any other structure, were removed. In some cases, the approximations of invert or offset values described above resulted in a negative or zero slope, indicating an overestimation of the unknown value. There are tools available in PCSWMM to automatically modify conduit slopes, but the over-utilization of these

tools would have overridden much of the known invert and slope values, negating the value of the tool's efficiency. Instead, the invert approximations that caused negative or zeros slopes were manually adjusted to preserve neighboring data. The decision-making framework could not be applied to areas in the stormwater network with clusters of structures with unknown details. These clusters were removed and it was assumed that the runoff the surrounding area would enter the minor system at the nearest known downstream inlet. Though simplifying the network may have led to localized errors in the overland flow the overall inputs to the minor system were not expected to be significantly altered. The contributing areas to the simplified network are relatively small and typically isolated on private property such as the Denver University campus where roadway flooding is not a concern for this study.